Materials Research Proceedings 54 (2025) 274-283 https://doi.org/10.21741/9781644903599-30

Framework for determining and simulating tensile properties of smart composite FDM printed parts

Mohamed Khalil Homrani[1,a *], Anthonin Demarbaix[2], Imi Ochana[1,2], and François Ducobu[1]

[1]Machine Design and Production Engineering Lab, Research Institute for Science and Material Engineering, University of Mons, Mons, Belgium

[2]Science and Technology Research Unit, Haute Ecole Provinciale de Hainaut Condorcet, Boulevard Solvay 31, 6000 Charleroi, Belgium

[a]mohamedkhalil.homrani@umons.ac.be

Keywords: Finite Element, Tensile Testing, Equivalent Materials, 3D Printing

Abstract. Fused deposition modeling (FDM) is an additive manufacturing technique with good precision and moderate tolerances. Utilizing Finite Element Analysis (FEA) in literature is now key to studying the properties of these printed parts. The nature of the FDM process results in anisotropic inner structures with microscopic voids that are heavily affected by printing parameters. Even more so than the latter, composite coextrusion FDM printed parts possesses anisotropy due to the joining of the two filaments in the melt phase. These effects need to be examined and incorporated in an adequate digital twin. There exists a valid alternative to simulating this complex anisotropy, with the creation of Equivalent Homogenized Material. This study aims to bridge the gap between experimental data and FEA models for smart composite FDM parts. The goal is to establish a framework for determining effective homogenous mechanical properties of said parts. The Rule of Mixtures (ROM) method is first examined, and the limitations quickly become apparent, as the method fails to distinguish between two study cases with similar volume fractions but different fiber/matrix layouts. The second method, Representative Volume Elements (RVE), does not possess such a disadvantage. With an adequate convergence study on RVE size and fiber distribution, the calculated equivalent material's properties show good agreement with experimental results, at a greatly increased computation cost.

Introduction

Additive Manufacturing (AM) has grown into a market worth over $4 billion back from the 1980s to 2015. Predictions estimate that the market cap has reached $35.6 billion in 2024 [1]. A lot of this growth can be attributed to research breakthroughs, from new AM materials to techniques that allow for cost cutting by making development faster and easier [2]. When combined with available digital tools such as topology optimization, digital twins and FEA models, progress can be made much cheaper and quicker than before. Allowing AM to transition into the production of dependable, application-ready goods.

Material Extrusion (MEX) is one of the 7 classes of AM, defined in ASTM F2792−12a, the standard for additive manufacturing technologies terminology. In this category of AM, material is selectively deposited through a nozzle to build a part layer by layer. The most popular technology within this class is Fused Deposition Modeling (FDM), in which polymers and polymer composites are most commonly used [3]. Recent advancements in composite FDM have extended its utility by incorporating reinforcing fibers, such as carbon or glass, into the thermoplastic matrix. These fiber-reinforced composites exhibit improved mechanical properties, such as tensile strength. Making FDM into a viable option for industrial grade applications.

Materials Research Proceedings 54 (2025) 274-283 https://doi.org/10.21741/9781644903599-30

Understanding the mechanical properties of these materials is crucial for the evolution of FDM. Several researchers have examined these characteristics and how they vary with print settings. Jung et al. [4] investigated the fatigue performance of Carbon Fiber Reinforced Plastics (CFRP). Different orientation angles of the carbon fiber were tested. Fatigue life was estimated through experimental testing, FEA fatigue analysis simulated the failure of these parts precisely.

While all mechanical properties are important for a complete understanding of composite FDM parts, tensile properties are the most researched mechanical property. It is the highest tensile stress that a material can sustain before failing. To enhance the printing process and obtain the required part qualities, it is crucial to comprehend the factors that affect it. ASTM D638 types I to IV geometries are used in these studies [5]. The American Society for Testing and Materials (ASTM) created this standard, which is used to assess the tensile characteristics of plastic materials.

Some studies in literature focus on these tensile properties, such as Allouch et al. [6] which use FDM to produce samples from Short Carbon Fiber reinforced Polyether Ether Ketone (CF/PEEK) filament. The impact of print orientation on the mechanical characteristics of the samples was validated through experimental results of Young's modulus, total elongation at failure, yield, and ultimate strength. The effects of carbon fiber length and content in FDM of CFRP samples were investigated by Ning et al. [7]. where carbon fiber powder was added to plastic pellets, which resulted in a 30% improvement in tensile mechanical properties. Tian et al. [8] studied the mechanical characteristics of CFRP samples. By testing various carbon fiber percentages, the authors optimized the appropriate fiber content for maximal flexural and tensile strength.

These studies show the need for material homogenization, which allows for the simplification of composite material microstructures into uniform representations with effective properties. This is necessary because these printed parts often have complex internal structures that are too computationally expensive to model directly. Homogenization provides average properties, enabling manageable simulations that still accurately predict overall behavior. Fig. 1 shows the convergence of effective material properties between homogenization techniques and experimental testing.

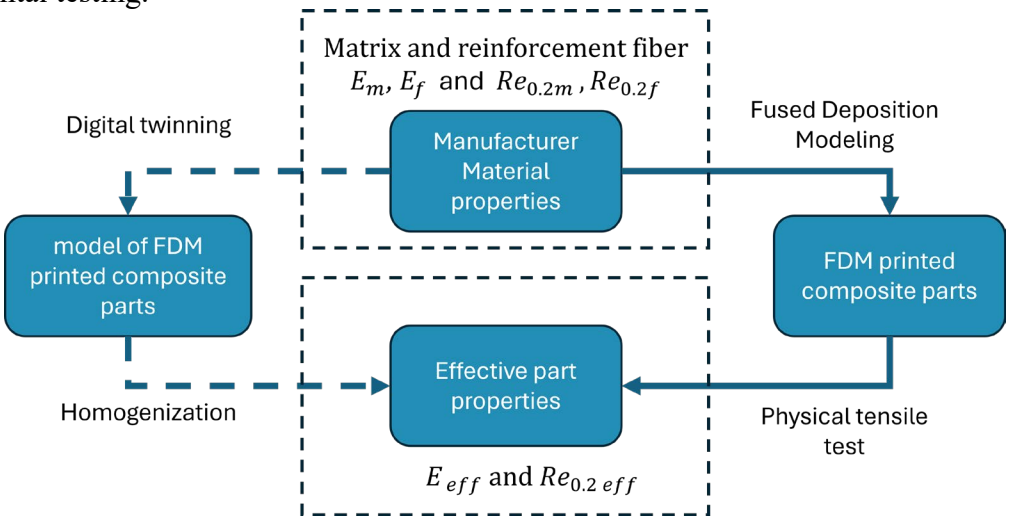

Figure 1 – Schematic explanation of effective material properties and the need for experimental validation of composite printed parts digital twins.

While FDM composites possess excellent mechanical properties, the layered nature inherent to the printing process results in manufacturing defects. Voids, variations in material density, or inadequate interlayer bonding often arise. Traditional inspection methods to minimize the effects of these defects are time consuming, costly, and prone to human error. Consequently, the integration of Structural Health Monitoring (SHM) methodologies within the context of FDM AM presents a significant advancement in quality assurance and performance assessment. The

implementation of SHM, employing embedded or surface-mounted sensors, offers a means for detection and characterization of these defects. This monitoring facilitates early detection of potential failure, therefore mitigating the risk of material failure and enhancing the long-term reliability of FDM fabricated parts [9].

Advanced digital twins and numerical models have been developed to effectively utilize SHM collected data from FDM parts. In simplified models, the infill and composite layouts in FDM parts are often represented as a network of beams, while the outer contour is modelled using shell elements. While mathematically insightful, this approach struggles to accurately represent complex geometries. Garg et al. [10] proposed a method that closely simulates the layer-by-layer and line-by-line deposition characteristic of FDM printing. However, discretizing each individual line with a sufficient number of elements results in a computationally intensive mesh, demanding substantial computing resources and time, even for relatively simple geometries. The present approach addresses this limitation by constructing a model based on internal imaging analysis of the component's mesostructure. Finding means of simplifying these material models that capture the heterogeneous nature of these materials while maintaining their accuracy is of high importance [11]. This is achieved through various mathematical models, such as the use of representative volume elements (RVEs) and constitutive laws derived from micromechanics principles, such as the rule of mixtures, enabling detailed simulations of material behavior and damage progression while minimizing costs for computation.

This study investigates the development of digital twins for AM carbon fiber-reinforced thermoplastic composites with integrated SHM. A Design of Experiments (DoE) methodology was employed to obtain sufficient data for experimental validation, varying key printing parameters: fiber filling patterns (U-shaped and W-shaped configurations) and number of fiber layers (two or four). Tensile testing was performed to characterize the mechanical behavior, specifically Young's modulus and yield strength. These experimental results serve as the basis for developing and validating a Finite Element Model (FEM) of the printed specimens. To simplify the modelling of these complex FDM composite structures, two distinct methodologies are compared: a simplified approach based on the rule of mixtures and a more detailed approach utilizing representative volume elements (RVEs). By comparing the predictions of these two modelling strategies with the experimental data obtained from the physical specimens, this study aims to provide a framework for determining equivalent material properties, as well as the most effective and computationally efficient method for creating accurate digital twins from the mechanical behavior of these SHM-integrated composites under tensile loading.

Experimental methodology and simulation setup

Tensile testing specimens were printed on the Anisoprint Composer A4 FDM coextrusion printer, according to the ASTM D638 type I standard geometry [5] using continuous CFRP composites. In total, 4 sets of specimens, consisting of 3 samples each were printed, the general print settings of which are detailed in Table 1. The coextrusion process was used to integrate the continuous carbon fibers within the thermoplastic matrix. Tensile tests were conducted using the Zwick/Roëll Z2.5 universal testing machine at a speed of 0.05 mm/s and a maximum force of 2500 N, with specimens securely clamped to prevent off-axis loading. Stress-strain data were recorded until failure to determine Young's modulus (E) and yield strength ($Re_{0.2}$), the tensile testing machine is shown in Fig. 2(a).

The simulation process of the tensile test is recreated using ABAQUS/Explicit finite element code. In total, four FE models were developed. Each model consists of a deformable dog-bone specimen in accordance with ASTM D638 type I geometry, the specimen geometry dimensions are shown in Fig. 2(b). while basic simulation parameters and loads are shown respectively in Fig. 2(c).

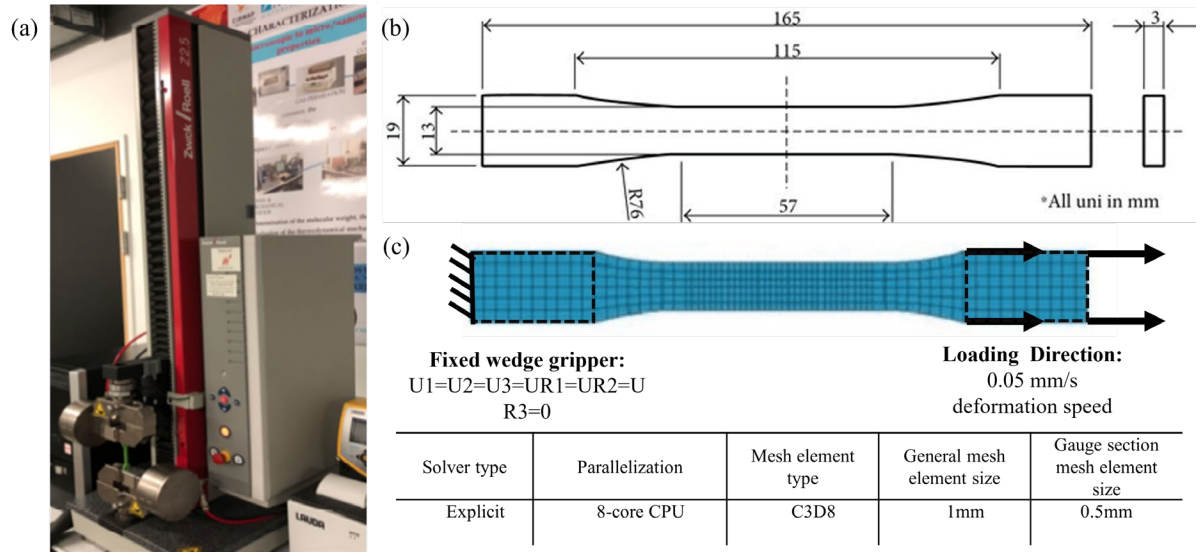

Solver type	Parallelization	Mesh element type	General mesh element size	Gauge section mesh element size
Explicit	8-core CPU	C3D8	1mm	0.5mm

Figure 2 – Zwick/Roëll Z2.5 universal testing machine (a), ASTM D638 type I standard geometry (b), and ABAQUS/Explicit simulation settings and boundary conditions (c).

Table 1 – General printing parameters for the dog-bone specimen.

Layer Thickness	T° Extrusion	T° Plate	T° maximum	Matrix Material	Reinforcement material
0.09mm	265° C	60° C	270° C	Anisoprint Smooth PA	CCF-1.5K Carbon composite fiber
Reinforcement material print nozzle	matrix print nozzle	Infill method	Infill percentage	Matrix extrusion speed	Reinforcement material extrusion speed
0.8mm	0.4mm	Isogrid	30%	45 mm/sec	3 mm/sec

All samples considered are printed with 30% infill density which is repeated across all sample group names. The U and W in the sample groups' designations is the number of passes through the gauge cross-section, respectively 2 and 4 passes. The 2 and 4 represent the number of layers of deposited reinforcement material in each pass, these sample group specific print settings are shown in Table 2 and further explained in Fig. 3. For further validation of the experimental results, a central set of samples was created. This M320 sample has three layers each of continuous carbon fiber with a 20% infill density. The fibers in each layer go back and forth three times. This setup is the middle point of the things we studied and is used as a starting point to see how changes in fiber patterns, number of layers, and matrix density affect the material.

Table 2 – Sample group specific printing parameters for the dog-bone specimen

Sample groups	Sample number	Carbon fiber filling pattern	Number of carbon fiber layers	E (MPa)	$Re_{0.2}$(MPa)
U230	1	U	2	2015.79	30.17
	2			1989.90	32.49
	3			2110.20	32.56
W230	1	W	2	2282.38	32.47
	2			2187.25	31.74
	3			2363.98	32.68
U430	1	U	4	2844.65	39.58
	2			2684.99	35.81
	3			2716.37	39.56
W430	1	W	4	3103.58	50.04
	2			3171.77	39.26
	3			3038.27	44.28

Samples highlighted in the table show anomalous Young modulus (E) and yield strength ($Re_{0.2}$) values. These values are not to be considered according to experimental calculation of the gauge factor (GF) which is the ratio of relative change in electrical resistance to the mechanical strain, unique to SHM-integrated parts. While most samples exhibited good consistency with an average R^2 of 0.99 and a variation of 2%, the highlighted anomalies were still observed and eliminated. In the U230 sample group, only specimen 3 of U230 provided reliable measurements, with a GF of 0.922 and an R^2 of 0.965. Similarly, only specimen 2 of sample group U410 was consistent, which showed a GF of 0.57 and an R^2 of 0.97.

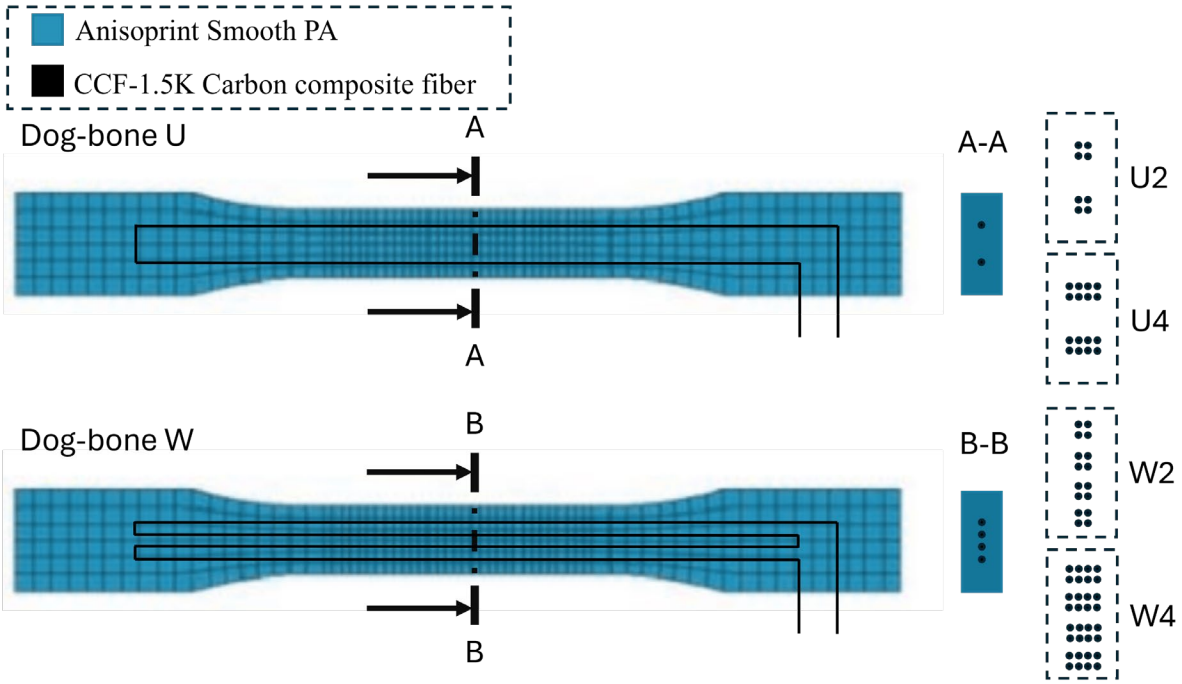

Figure 3 – Sample group names schematic explanation, carbon fiber reinforcement material layout (U or W) and number of carbon fiber reinforcement layers (2 or 4).

Materials Research Proceedings 54 (2025) 274-283 https://doi.org/10.21741/9781644903599-30

Material homogenization

Material homogenization is used to simplify the complex heterogeneous nature of the printed FDM composite parts into a homogeneous representation with effective properties. As previously explained, directly modeling microstructure details within a full-scale FEA of a specimen presents significant computational challenges. Therefore, homogenization provides a necessary simplification, enabling efficient simulations while retaining sufficient accuracy for predicting overall mechanical behavior as shown in Fig. 4.

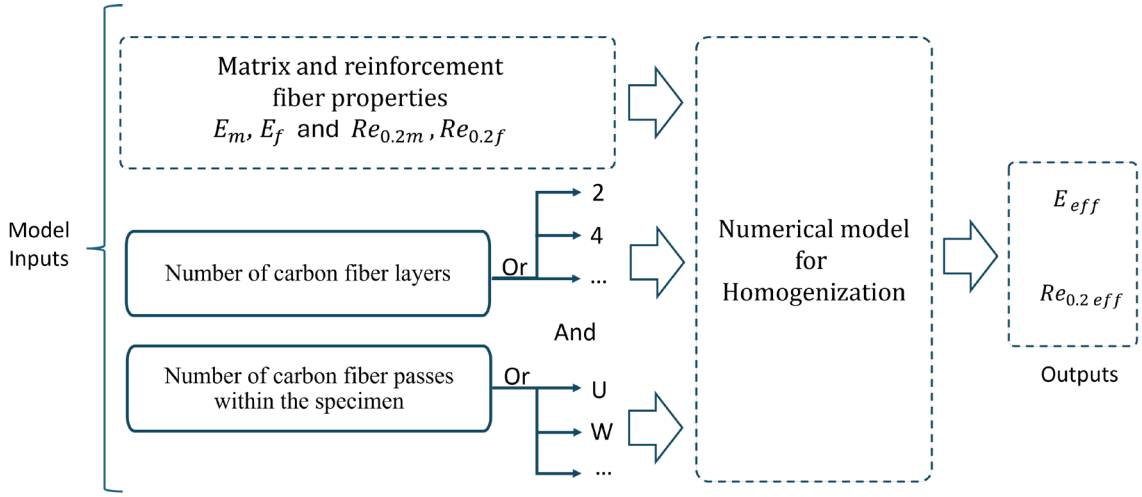

Figure 4 – The use of material homogenization for the determination of effective material properties in FDM printed composites.

Material homogenization, in its simplest form, can be represented by the Rule of Mixtures (ROM) as shown in Eq. 1 [12] which is used for calculating the Young modulus of composites with a unidirectional fiber orientation and continuous fibers. ROM assumes perfect bonding between the reinforcement fibers and matrix constituents. and either uniform stress or strain distributions. While ROM offers a computationally inexpensive method for obtaining initial estimates of effective properties, its limitations are well documented, particularly for discontinuous fiber composites like those produced by FDM. The presence of voids, imperfect interfaces, and non-uniform fiber distribution significantly deviates from the idealized assumptions of ROM, leading to inaccuracies in property predictions. Consequently, more sophisticated homogenization techniques are required to accurately capture the mechanical behavior of FDM composites.

$$E_{eff} = V_f . E_f + V_m . E_m, \tag{1}$$

where E is Young modulus, V is volume fraction, and the subscripts eff, f and m are effective, fibers and matrix, respectively. For composites with non-unidirectional fiber orientations and discontinuous fibers, a combined rule of mixtures model is commonly used which is not necessary in this case. These ROM models however possess low porosity ($V_f + V_m = 1$). Thus, for composites containing a significant amount of porosity, which is the case for 30% infill density FDM printed parts, the equations are inappropriate for calculating the mechanical properties of the composite. The input parameters for the ROM model will be evaluated. Following this, a porosity-corrected rule of mixtures model, explicitly accounting for all three volume phases (fiber, matrix, and voids).

Prior work has shown that incorporating the factor $(1 - V_p)^n$ into the rule of mixtures model effectively simulates the influence of porosity on plant fiber composite stiffness [12] resulting in Eq. 2. The parameter n represents the porosity efficiency exponent, quantifying the stress concentration effects of porosity within the composite. When n is zero, the effect of porosity is

eliminated. This porosity correction approach is consistent with similar methods used in a study [12]. Where the effects of spherical voids in materials are studied.

$$E_{eff} = \left(1 - V_p\right)^n (V_f . E_f + V_m . E_m). \quad (2)$$

Fiber, matrix, and porosity volume fractions in composites are interdependent. Fig. 5 shows a detailed cross-section at the gauge of the U230 specimen.

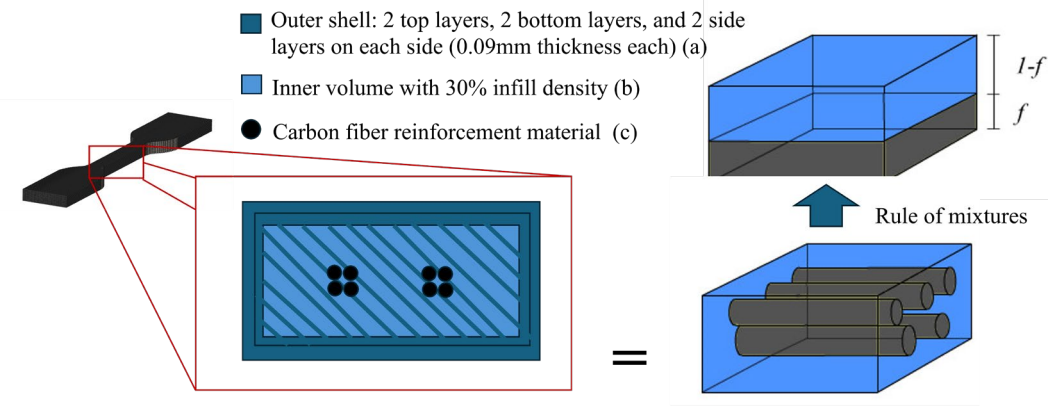

Figure 5 – Cross-section of a U230 specimen rule of mixtures (ROM) transformation, showing the solid outer shell (a), inner volume (b) and the carbon reinforcement fibers.

The volume fractions of fiber V_f, matrix V_m, and porosity $V_p$were determined through analysis of the cross-section presented in Fig. 5, these calculated values are shown in Table 3. Additionally, in order to determine the appropriate value for the porosity efficiency exponent (n) used in the porosity-corrected Rule of Mixtures, both the Sum of Squared Errors (SSE) and the Root Mean Squared Error (RMSE) were employed to compare the predicted effective properties with experimentally obtained values. This optimization process allowed for the identification of a singular n value that minimized the discrepancy between the model predictions and the experimental data. These calculated volume fractions and porosity efficiency exponent, in conjunction with manufacturer-provided mechanical properties for the constituent materials (fiber and matrix), which can then be utilized to estimate the effective Young's modulus E_{eff} and the 0.2% offset yield strength $R_{0.2eff}$ of the composite material as shown in Table 4.

Table 3 – Calculated volume fractions for fiber, matrix and pores.

Sample groups	RMSE Optimized porosity efficiency exponent (n)	Vf	Vm	Vp
U230	1.21	1.4%	33.9%	64.7%
W230	1.21	2.8%	32.5%	64.7%
U430	1.21	2.8%	32.5%	64.7%
W430	1.21	5.6%	29.7%	64.7%

A more robust approach is based on the Representative Volume Element (RVE). Which is a statistically representative volume of the composite microstructure, encompassing a sufficient number of fibers and matrix to capture the essential features of the material. The size of the RVE must be large enough to be statistically representative yet small enough to remain computationally efficient. Within the RVE, the actual microstructure is explicitly modeled, allowing for the consideration of fiber orientation, distribution, clustering, and the influence of the matrix phase. The RVE is then subjected to uniaxial tension. FEA is then performed on the RVE to determine

the resulting stress and strain fields. From these fields, effective material properties are derived through volume averaging techniques. A microscale RVE model was developed for each sample group to determine the orthotropic elastic properties of the FDM specimens. The converged upon RVEs, depicted in Fig. 6, contain the three phases: matrix, fiber, and void. These models were generated using ABAQUS/Explicit, with an Isogrid infill pattern, identical to the one sliced by Anisoprint Aura v2.5.7. Subsequent meshing and solution were performed using the ABAQUS/Explicit solver. Linear isotropic and linear transversely isotropic elastic material models were assumed for the Anisoprint Smooth PA matrix and CCF-1.5K Carbon composite fibers, respectively, with fiber volume fractions seen in Table 3 within the matrix. The mechanical properties of the Anisoprint Smooth PA matrix and CCF-1.5K Carbon composite fibers were obtained from supplier datasheets.

A mesh convergence study was conducted, resulting in a refined RVE mesh containing up to 218,733 elements. Boundary uniaxial tensile test conditions were applied in the fiber direction. This boundary condition enforced the necessary constraints and ensured periodicity of the stress and strain fields within the RVE [13]. Effective material properties were determined by applying a single loading mode in each simulation. Specifically, effective Young modulus and 0.2% offset yield strength were calculated by applying a normal strain in the same direction as the fiber.

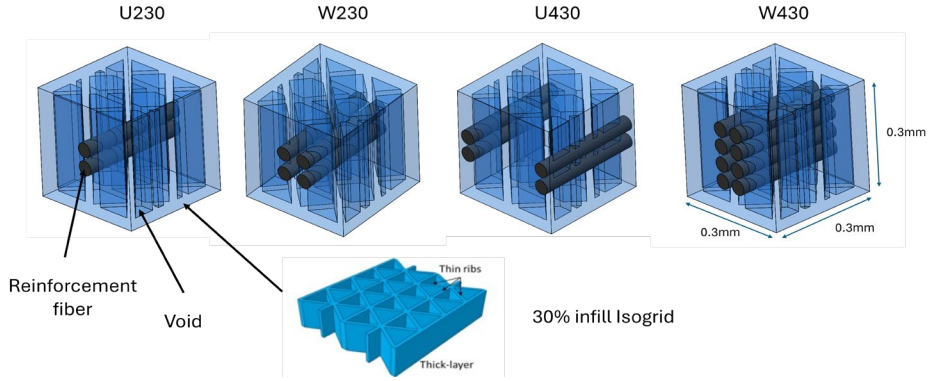

Figure 6 – Representative volume elements (RVEs) for each sample group.

During homogenization, the effective mechanical properties are sensitive to the relative size and distribution of the constituent phases within the RVE. Hince the need for a convergence study.

Table 4 – Calculated effective Young's modulus E_{eff} and the 0.2% offset yield strength $R_{0.2eff}$ of the composite material with prediction error in percentage.

Sample groups	Median Experimental E_{eff} (MPa)	ROM E_{eff} (MPa)	RVE E_{eff} (MPa)	Median Experimental $Re_{0.2eff}$ (MPa)	ROM $Re_{0.2eff}$ (MPa)	RVE $Re_{0.2eff}$ (MPa)	ROM Error (%)
U230	2110.20	2086.28	2212.34	32.56	32.19	33.11	1.13
W230	2277.87	2212.22	2254.56	32.47	31.53	32.83	2.88
M320	2428.44	2402.5024	2501.30	38.74	39.15	39.08	1.06
U430	2748.67	2212.94	2812.11	39.56	31.84	40.98	19.49
W430	3103.58	3074.67	3189.07	50.04	49.57	51.26	0.93

A convergence study was performed to assess the influence of RVE size and fiber placements on the predicted properties. In this study, all voids were as an isogrid infill pattern with 30% infill density. While maintaining a constant overall void volume fraction, the size of the RVE was varied first, encompassing different numbers of fibers for each sample group. Specifically, RVEs containing 1, 2,3, 4 and 8 fibers were analyzed. With different placements and bundles for the fibers each. Results of the simulated effective Young's modulus E_{eff} and the 0.2% offset yield

strength $R_{0.2eff}$ of the composite material are shown in Table 4 along with the results from the porosity-corrected ROM. Fig. 7 depicts the experimental stress/strain curves of U430 and W230, in comparison to the ROM and RVE models respectively. The limitation of ROM homogenization can be clearly seen, as the 2 different specimen groups generate identical Stress/strain curves despite having differing experimental results.

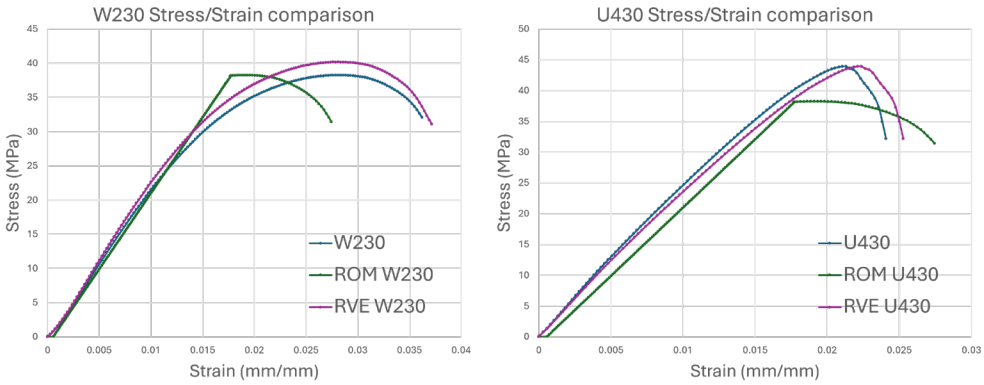

Figure 7 – Stress/strain Abaqus/explicit simulation results for ROM and RVE models compared with experimental results.

Conclusions

This study offers valuable insight into the applicability and limitations of ROM for predicting the mechanical behavior of smart FDM composite materials. While the ROM demonstrates reasonable predictive capability for certain sample groups. Significant discrepancies are still observed in sample group U430. When further analyzing this major discrepancy, it can be seen that the values of effective Young's modulus and the offset yield strength for both W230 and U430 are identical. This is a consequence of the limitations of the ROM. This discrepancy is significantly mediated by the more complex RVE method, which despite being more computationally demanding, allows for closer estimation of mechanical properties, even for such similar cases.

- Both groups W230 and U430 possess exactly 16 deposited reinforcement fibers. W230 being 4 passages of 4 fibers each, and U430 being 2 passages of 8 fibers each. This results in an identical set of volume fractions, resulting in a similar effective Young's modulus and yield strength of the composite material for both specimens when utilizing ROM.
- Load Distribution accurately explains the difference in values for experimental tensile results. When a tensile load is applied, it is distributed among the fibers. In the specimen with 4 bundles, the load is distributed across more bundles. This means each individual small fiber experiences a lower stress. Taking advantage of this in the creation of RVE, the issue is seemingly resolved with the resulting effective mechanical properties and Stress/Strain curves having better agreement with experimental results.
- Another valid explanation for this discrepancy in experimental results despite similar volume fractions of fiber and matrix are stress concentrations. The interfaces between the fiber bundles and the surrounding matrix material are areas where stress can concentrate. A higher number of interfaces promotes more uniform stress distribution and potentially increases overall tensile strength. The RVE method simulates this nuance by allowing freedom in fiber placements.

Acknowledgements

The authors would like to thank Région Wallonne for supporting this research as part of the SKYWIN ICOM2C3D research project under grant 8820.

References

[1] Terry T Wohlers and Tim Caffrey. Wohlers report 2019: 3d printing and additive manufacturing state of the industry annual worldwide progress report. 2019.

[2] Hu B, Duan X, Xing Z, Xu Z, Du C, Zhou H, Chen R, Shan B. Improved design of fused deposition modeling equipment for 3D printing of high-performance PEEK parts. Mechanics of Materials. 2019 Oct 1;137:103139. https://doi.org/10.1016/j.mechmat.2019.103139

[3] Mattey R, Jewell B, Ghosh S, Sain T. Phase-field fracture coupled elasto-plastic constitutive model for 3D printed thermoplastics and composites. Engineering Fracture Mechanics. 2023 Oct 26;291:109535. https://doi.org/10.1016/j.engfracmech.2023.109535

[4] Jung CH, Kang Y, Song H, Lee MG, Jeon Y. Ultrasonic fatigue analysis of 3D-printed carbon fiber reinforced plastic. Heliyon. 2022 Nov 1;8(11). https://doi.org/10.1016/j.heliyon.2022.e11671

[5] ASTM D638-14, "Standard Test Method for Tensile Properties of Plastics", American Society for Testing and Materials, doi: 10.1520/D0638-14. https://doi.org/10.1520/D0638-14

[6] Allouch M, Ben Fraj B, Dhouioui M, Kesssentini A, Hentati H, Wali M, Ferhi M. Mechanical, microstructural and numerical investigations of 3D printed carbon fiber reinforced PEEK. Proceedings of the Institution of Mechanical Engineers, Part C: Journal of Mechanical Engineering Science. 2024 Mar;238(6):2131-9. https://doi.org/10.1177/09544062231190534

[7] Ning F, Cong W, Qiu J, Wei J, Wang S. Additive manufacturing of carbon fiber reinforced thermoplastic composites using fused deposition modeling. Composites Part B: Engineering. 2015 Oct 1;80:369-78. https://doi.org/10.1016/j.compositesb.2015.06.013

[8] Tian X, Todoroki A, Liu T, Wu L, Hou Z, Ueda M, Hirano Y, Matsuzaki R, Mizukami K, Iizuka K, Malakhov AV. 3D printing of continuous fiber reinforced polymer composites: development, application, and prospective. Chinese Journal of Mechanical Engineering: Additive Manufacturing Frontiers. 2022 Mar 1;1(1):100016. https://doi.org/10.1016/j.cjmeam.2022.100016

[9] Modir A, Tansel I. Analysis of force sensing accuracy by using SHM methods on conventionally manufactured and additively manufactured small polymer parts. Polymers. 2022 Sep 8;14(18):3755. https://doi.org/10.3390/polym14183755

[10] Garg A, Bhattacharya A. An insight to the failure of FDM parts under tensile loading: finite element analysis and experimental study. International Journal of Mechanical Sciences. 2017 Jan 1;120:225-36. https://doi.org/10.1016/j.ijmecsci.2016.11.032

[11] Anoop MS, Senthil P. Homogenisation of elastic properties in FDM components using microscale RVE numerical analysis. Journal of the Brazilian Society of Mechanical Sciences and Engineering. 2019 Dec;41:1-6. https://doi.org/10.1007/s40430-019-2037-8

[12] R.J. Ong, J.T. Dawley and P.G. Clem: submitted to Journal of Materials Research (2003). https://doi.org

[13] van de Werken N, Koirala P, Ghorbani J, Doyle D, Tehrani M. Investigating the hot isostatic pressing of an additively manufactured continuous carbon fiber reinforced PEEK composite. Additive Manufacturing. 2021 Jan 1;37:101634. https://doi.org/10.1016/j.addma.2020.101634